

Origin of Intermittent Plastic Flow and Instability of Shear Band Sliding in Bulk Metallic Glasses

B. A. Sun,^{1,*} S. Pauly,¹ J. Hu,² W. H. Wang,³ U. Kühn,¹ and J. Eckert^{1,4}

¹*IFW Dresden, Institut für Komplexe Materialien, Helmholtzstraße 20, D-01069 Dresden, Germany*

²*School of Material and Mechanical Engineering, Beijing Technology and Business University, Beijing 100048, China*

³*Institute of Physics, Chinese Academy of Sciences, Beijing 100080, China*

⁴*TU Dresden, Institut für Werkstoffwissenschaft, Helmholtzstraße 7, D-01069 Dresden, Germany*

(Received 27 November 2012; published 30 May 2013)

Intermittent or serrated plastic flow is widely observed in the deformation of bulk metallic glasses (BMGs) or other disordered solids at low temperatures. However, the underlying physical process responsible for the phenomena is still poorly understood. Here, we give an interpretation of the serrated flow behavior in BMGs by relating the atomic-scale deformation with the macroscopic shear band behavior. Our theoretical analysis shows that serrated flow in fact arises from an intrinsic dynamic instability of the shear band sliding, which is determined by a critical stiffness parameter in stick-slip dynamics. Based on this, the transition from serrated to nonserrated flow with the strain rate or the temperature is well predicted and the effects of various extrinsic and intrinsic factors on shear band stability can be quantitatively analyzed in BMGs. Our results, which are verified by a series of compression tests on various BMGs, provide key ingredients to fundamentally understand serrated flow and may bridge the gap between the atomic-scale physics and the larger-scale shear band dynamics governing the deformation of BMGs.

DOI: [10.1103/PhysRevLett.110.225501](https://doi.org/10.1103/PhysRevLett.110.225501)

PACS numbers: 61.43.Dq, 62.20.F-, 81.05.Kf

Despite different length scales and internal dynamics, a variety of disordered materials ranging from granular media and colloids to metallic glasses exhibit remarkably similar shear localization and intermittent plastic flow behavior when deformed at low temperatures [1–3]. In view of the fundamental interest in the structure-property relationships of disordered materials and their wide applications, there is a compelling need to identify the physical processes underlying the plastic flow of these materials. At atomic scale, the plastic flow of glassy materials is believed to involve the local arrangement of atomic clusters that undergo inelastic deformation [4–6], which is completely different from dislocation-mediated plasticity in crystalline solids. Several theoretical models including the free volume [7] and the shear transformation zone (STZ) theory [8–10] were proposed over the years, providing a comprehensive interpretation to the plasticity of glassy materials. Despite the success of these theories in understanding the fundamental flow process and the rheological behavior [11–13], demonstrating the macroscopic deformation behavior with these microscopic theories still presents a major challenge in glassy materials.

This dilemma particularly stands out in bulk metallic glasses (BMGs), a new class of disordered materials that have gained much attention owing to their attractive and unique properties [14–16]. At temperatures far below the glass transition, the plastic deformation of BMGs is well known to be an inhomogeneous process with the plastic strain highly localized into shear bands [17,18]. According to the free volume approach or the STZ theory, this shear

localization can be illustrated as a spatial instability process by a softening mechanism associated with structural disordering or shear dilation, and once a shear band is initiated, it will quickly reach a steady state with a largely reduced viscosity [8,19]. However, in contrast to the prediction, the intermittent shear banding process often occurs, which is widely observed in load-constraint deformation modes and manifested as serrated flow behavior in the stress-strain curves [20–22]. Similar intermittent flow behavior has also been reported for a variety of other disordered materials [1–3]. Regarding the significant softening, it is difficult to understand why shear banding is arrested and then reactivated during serrated flow. Although some mechanisms have been suggested, including nanocrystallization within shear bands [23] and repeated shear-melting transition [24], the physical mechanism of serrated flow, particularly from the fundamental deformation process of BMGs, remains a mystery. Furthermore, serrated flow shows a strong dynamic dependence on the strain rate and the temperature, i.e., serrations tend to be suppressed at high strain rates or low temperatures and disappear at some critical values [25–28]. The physical mechanism for the dynamic characteristic is also poorly understood.

In this letter, we attempt to interpret the intermittent plastic flow in BMGs by relating their atomic-scale deformation process and macroscopic shear band behavior. There are many theoretical models to describe the atomic-scale deformation process of BMGs. Here, we use the cooperative shearing model (CSM) of STZs recently

proposed by Johnson and Samwer [10]. The CSM is mainly based on the concept of inherent states and the potential energy landscape [29] and considers that the mechanical instability of a STZ is related with the stress-induced destabilization of individual inherent state or local minima of potential energy landscape in BMGs. Thus, a correlation between structure of metallic glasses and their energetics can be well established. According to the CSM, the potential energy barrier for the instability of a STZ is biased by an applied shear stress. The inelastic strain rate for crossing the barrier is expressed as:

$$\dot{\gamma} = \dot{\gamma}_s \exp(-W_\tau/k_B T), \quad (1)$$

where $\dot{\gamma}_s$ is a characteristic strain rate, k_B is the Boltzmann constant, T is the temperature and W_τ is the energy barrier to overcome at a finite shear stress τ . From the Frenkel scheme for shear deformation of dislocation-free crystals and the catastrophe theory, it is easily shown that $W_\tau = 4RG_{0T}\gamma_C^2[(\tau_C - \tau)/\tau_C]^{3/2}\zeta\Omega$ [10] where G_{0T} is the shear modulus of the unstressed glass, $\gamma_C \approx 0.027$ and τ_C is the critical yield shear strain and stress of a BMG, respectively, Ω is the volume of a STZ, $R \approx 1/4$ and $\zeta \sim 2-4$ are constants. Thus, Eq. (1) in fact gives a constitutive description of the plasticity from the atomic-scale deformation physics in amorphous solids. Following the CSM, the universal $T^{2/3}$ temperature dependence of the yield strength in BMGs has been well elucidated and the volume of STZs for various BMGs can be experimentally characterized [30].

To relate the atomic-scale process with the macroscopic deformation behavior, we consider the uniaxial compression of a BMG. In this case, most monolithic BMGs will deform by the formation of a dominant shear band along the principle shear plane, as shown in Fig. 1. The machine-sample system (MSS) is loaded at a constant rate v_0 from

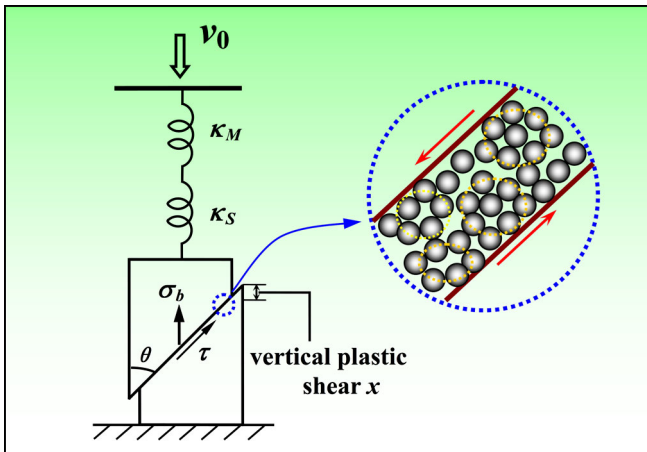


FIG. 1 (color online). Schematic diagram of the machine-sample system in the compression of BMGs where a dominant shear band is formed. The shear banding can be viewed as cooperative shear process of a collection of STZs, as shown in the schematic atomic-scale process in the band.

the time $t = 0$, and elastic energy is gradually stored in the system providing the driving force $\kappa_M \kappa_S v_0 t / (\kappa_M + \kappa_S)$ with κ_M and κ_S being the stiffness of the machine and the sample, respectively. Once the sample is loaded up to the yield stress, the major shear band will form. After activation, the band will quickly operate across the entire sample and subsequent shearing proceeds in a cooperative manner [22]. For a vertical plastic shear displacement x in the band, the governing kinetic equation for the MSS is

$$\frac{\kappa_M \kappa_S}{\kappa_M + \kappa_S} (v_0 t - x) - \frac{\pi d^2}{4} \sigma_b = M \ddot{x}, \quad (2)$$

where d is the sample diameter, \ddot{x} is the second time derivative of x , and M is the effective inertia of MSS, typically on the order of 10–100 kg [31]. σ_b is the internal resistant stress of the shear band, which can be given by the constitutive law of the BMG. Defining the elastic constant

$$k = \frac{4\kappa_M \kappa_S}{\pi d^2 (\kappa_M + \kappa_S)} = \frac{E}{L(1+S)}, \quad (3)$$

where L and E are the height and Young's modulus of the sample, respectively, and S is defined by $S = \kappa_S / \kappa_M = \pi d^2 E / (4L \kappa_M)$, Eq. (2) becomes

$$k(v_0 t - x) - \sigma_b = m \ddot{x}, \quad (4)$$

with $m = 4M / \pi d^2$. Here, k and m can be regarded as the stiffness and the inertia of the system per unit area, respectively. From Eq. (4), one can see that the intermittent sliding of shear band will cause flow serrations in the load-displacement curve (Fig. S1 in the Supplemental Material [32]). In a serration, the deforming band will undergo negligible ($v \ll v_0$) and rapid ($v \gg v_0$) sliding rates. As indicated in recent works [33], this behavior is a typical stick-slip process [34,35], a phenomenon that has been widely observed in a large number of systems ranging in scale from atomic thin films to earthquake faults and differing vastly in their internal physics. For BMGs with multiple shear bands, similar stick-slip dynamic equations could also be derived by considering the interplay between shear bands [22,31].

In order to link the CSM with the stick-slip dynamics of shear band, we view shear banding as a cooperative shear of a thin layer where the constitutive deformation law can be described by the STZ theory. Because of the small thickness and extremely high strain rate in the shear band, we assume that the strain rate $\dot{\gamma}$ in the band is macroscopically homogeneous. Equation (1) can generally give a constitutive relation of the strain rate as a function of the applied shear stress τ during the deformation of BMGs. However, to fully describe the dynamics of shear band, we note that $\dot{\gamma}$ is also a function of some state variable in addition to the applied stress. Here, we use the concept of the effective disorder temperature χ proposed by Langer [36] as the state variable in the band. In STZ theory, χ is used to characterize the state of configuration disorder and

the density or the total number of STZs is proportional to the Boltzmann factor $\exp(-1/\chi)$. As the macroscopic strain rate $\dot{\gamma}$ in the band is proportional to two factors: the strain rate of the individual STZ and the number of STZs contained in the band, it can be expressed as $\dot{\gamma} = \exp(-1/\chi)f(\tau)$ with $f(\tau)$ given by Eq. (1). χ also evolves dynamically with the strain rate during deformation. We adopt a governing dynamic equation for χ [37]:

$$\dot{\chi} = \frac{\dot{\gamma}\tau}{c_0\tau_C} \left(1 - \frac{\chi}{\hat{\chi}(\dot{\gamma})}\right), \quad (5)$$

where c_0 is a constant, $\dot{\gamma}\tau$ is the energy dissipation term when the plastic work is done on the system, $\hat{\chi}(\dot{\gamma})$ is the steady state value of χ , which is a function of the plastic strain rate. The $\hat{\chi}(\dot{\gamma})$ can be given by $\hat{\chi}(\dot{\gamma}) = \chi_w / \ln(q_c/\dot{\gamma})$ from simulation results of a glass [38], where q_c is the characteristic strain rate that the effective temperature diverges and χ_w is the activation energy barrier which determines the frictional rate dependence. If $\chi_w < 1$, the material is rate weakening which means that the steady-state shear stress increases with strain rate. Here we assume that $\chi_w < 1$ always holds. As shown in Supplemental Materials [32], this is the prerequisite for the instability of steady shear band sliding to occur. Finally, the shear stress τ and the strain rate $\dot{\gamma}$ in the band are related to the vertical stress σ_b and the sliding rate v by the geometrical relations $\tau = \sigma_b \sin\theta \cos\theta$ and $\dot{\gamma} = v/(\lambda_b \cos\theta)$, where θ and λ_b are the shear band angle and thickness, respectively. Inserting these relations into the expression of $\dot{\gamma}(\chi, \tau)$ and rewriting it, we obtain a constitutive friction law of the shear band:

$$\sigma_b(v_0, \chi) = \sigma_{b0} \{1 - (kT/W_0)^{2/3} [\ln(v_s/v) - 1/\chi]^{2/3}\}, \quad (6)$$

where $\sigma_{b0} = 2\tau_C/\sin(2\theta)$, $v_s = \dot{\gamma}_s \lambda_b \cos\theta$, and $W_0 = 4RG_{0T}\gamma_C^2\xi\Omega$. Thus, the sliding of shear band is analogous to the solid friction process with a state variable friction in the planar interface (Fig. S2 in the Supplemental Material [32]).

With Eqs. (4)–(6), the stability of shear band sliding can be analyzed. Apparently, Eq. (4) has a steady-state solution $x^{SS} = v_0 t - \sigma_b^{SS}(v_0)/k$, where the shear band slides at the constant loading rate v_0 , and σ_b and χ reach their steady values $\sigma_b^{SS}(v_0)$ and $\hat{\chi}(v_0)$, respectively. This corresponds to the case of nonserrated or smooth flow in the plastic stress-strain curve of BMGs usually observed at low temperatures [25]. However, this steady sliding of shear band is not always stable. We perturbed these solutions and then performed linear stability analysis (see the Supplemental Material [32]). The analysis shows that the stability of the steady sliding is associated with a finite critical stiffness k_{cr} which is a function of the external loading rate v_0 and the temperature T :

$$k_{cr}(v_0, T) = \alpha \sigma_{b0} (k_B T/W_0)^{2/3} \ln(v_c/v_0)/C_0, \quad (7)$$

where $v_c = q_c \lambda_b \cos\theta$, $C_0 = (3/2)c_0 \lambda_b \cos\theta \chi_w^2/(1 - \chi_w)$ and α are constant factors. For $k > k_{cr}$, the initial perturbation on the steady shear band sliding will decay exponentially with time and, consequently the steady sliding is stable. Conversely, for $k < k_{cr}$, the small initial perturbation grows exponentially, leading to instability of the steady sliding. As shown from numerical solutions on the dynamic equations (see Figs. S4 and S5 in [32]), the instability will finally develop into stable serrations with fixed amplitude and duration. In this case, the calculated stress drop amplitude and the incubation time for slip events are found to be closely related to the ratio k/k_{cr} , which depends on various properties of BMGs as well as the loading rate and the testing temperature. Hence, serrated flow can be regarded as an intrinsic dynamic instability of the steady-state shear band sliding in BMGs.

According to Eq. (7), maps for the transition from serrated to nonserrated flow in BMGs can be plotted as a function of the loading rate v_0 or the testing temperature T , as shown in Fig. 2. One can see that k_{cr} decreases logarithmically with v_0 for constant T or increases with $T^{2/3}$ for constant v_0 . At $k = k_{cr}$, the transition occurs, where a critical rate v_{cr} or temperature T_{cr} can be found. For $v_0 > v_{cr}$ or $T < T_{cr}$, $k > k_{cr}$, the steady sliding is stable and hence nonserrated flow is observed. This explains experimental observations that serrations tend to be suppressed at

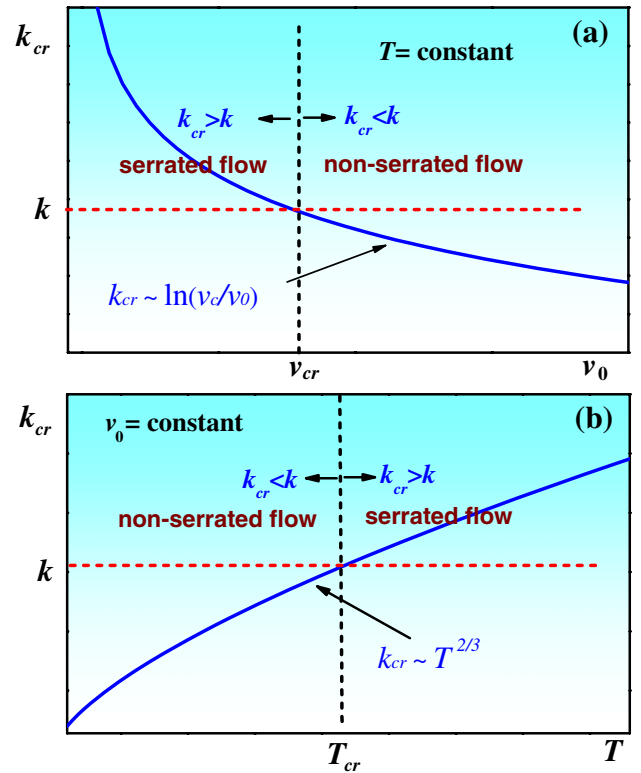


FIG. 2 (color online). The transition map from serrated to nonserrated flow at a constant temperature T (a) and a constant loading rate v_0 (b), respectively.

higher strain rates or lower temperatures [25,26]. Combining Eqs. (3) and (7) and considering the relation for the strain rate $\dot{\epsilon} = v_0/L$, one can obtain the critical strain rate for the disappearance of serrated flow

$$\dot{\epsilon}_{cr} = \dot{\epsilon}_c \exp\left[-\frac{C_0 k}{\alpha \sigma_{b0}} \left(\frac{W_0}{k_B T}\right)^{2/3}\right], \quad (8)$$

where $\dot{\epsilon}_c = v_c/L$. As $k = E/[L + \pi d^2 E/(4\kappa_M)]$, one can see that $\dot{\epsilon}_{cr}$ depends on the size and the Young's modulus of BMG samples as well as the testing temperature and machine stiffness. Thus, Eq. (8) provides a quantitative description on the dynamic transition of serrated flow and a theoretical basis for analyzing the effects of extrinsic (strain rate, sample size, etc.) or intrinsic (elastic modulus) factors on serrated flow and shear band stability in BMGs.

To verify our predictions, we performed a series of compression tests for various BMG samples with different sizes and elastic constants as listed in Table SI [32]. The machine stiffness κ_M in the present work is experimentally determined as $1.752 \times 10^7 \text{ N m}^{-1}$ (Fig. S6 [32]). Based on these parameters, the values of k were calculated according to Eq. (3) and are also listed in Table SI in the Supplemental Material [32]. For each sample, the critical loading rate v_{cr} or, equivalently, the critical strain rate $\dot{\epsilon}_{cr}$ for the transition from serrated to nonserrated flow can be experimentally determined by varying the strain rate in the tests at a constant temperature. The detailed procedure for determining the critical strain rate can be found in experimental methods and Fig. S7 in the Supplemental Material. Here, we choose $T = 218 \text{ K}$, as $\dot{\epsilon}_{cr}$ for most BMGs lie in the quasistatic range at this temperature (see Table SI), where serrations can be well resolved by our experimental setup (Fig. S8). Figure 3 shows the transition map from serrated to nonserrated flow where the critical strain rate v_{cr} (within the error range) versus k can be fitted well by Eq. (7)

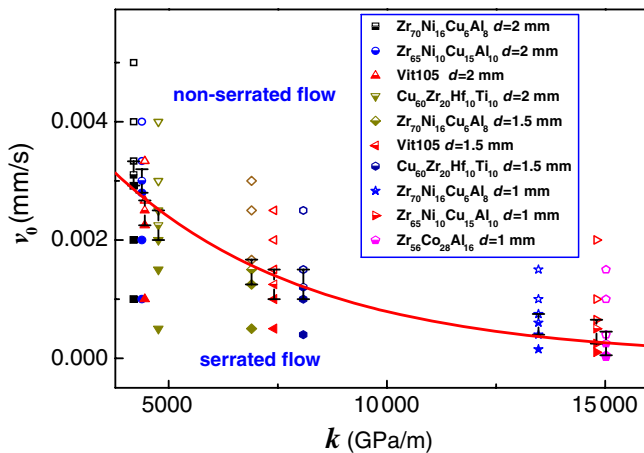


FIG. 3 (color online). The experimentally determined transition map from serrated to nonserrated flow for various BMGs with different sizes and elastic modulus at $T = 218 \text{ K}$, where the critical loading rate v_{cr} versus k can be fitted well by Eq. (7).

with the fitting constant $(W_0/k_B T)^{2/3} C_0/\alpha \sigma_{b0} = 2.21 \times 10^{-4} \text{ m GPa}^{-1} \text{ s}^{-1}$ for various BMGs. Alternatively, the critical strain rate also varies with the temperature T for a given MG sample with fixed k . In this case, Eq. (8) is reduced to a Super-Arrhenius relation

$$\dot{\epsilon}_{cr} = \dot{\epsilon}_c \exp[-Q(T)/k_B T] \quad (9)$$

with the activation energy $Q(T) = C_0 k W_0^{2/3} (k_B T)^{1/3} / (\alpha \sigma_{b0})$. Thus, the critical strain rate $\dot{\epsilon}_{cr}$ is inversely proportional to the exponential form of $T^{2/3}$. This temperature dependence of $\dot{\epsilon}_{cr}$ obviously originates from the $T^{2/3}$ dependence of the yielding stress of BMGs in the CSM model [10]. To verify this, we also performed compression tests on a typical $\text{Zr}_{65}\text{Cu}_{15}\text{Ni}_{10}\text{Al}_{10}$ BMG sample ($d = 2 \text{ mm}$) at different temperatures ($T \sim 203\text{--}298 \text{ K}$). At each temperature, the strain rate was gradually varied so that the transition from serrated to nonserrated flow is revealed, as shown in Fig. 4. One can see that the critical strain rate for the transition can be well fitted by Eq. (9) with the fitting activation energy $Q(T)$ in a narrow range of $0.53\text{--}0.58 \text{ eV}$ for T $203\text{--}263 \text{ K}$. Interestingly, a similar activation energy ($Q = 0.37 \text{ eV}$) for the serrated to nonserrated flow transition has also been obtained in recent compression experiments by Dubach *et al.* [25], where they fitted the data with an Arrhenius relation. All these results strongly corroborate our theoretical predictions and underpin the validity of the stick-slip instability in describing the dynamic characteristic of serrated flow in BMGs.

It should be noted that our model only considers the stick-slip dynamics of one single shear band and the prediction qualitatively agrees with the experimental facts that most monolithic BMGs deform by a dominant shear band where the serrations have a characteristic size [21]. For ductile BMGs, their serration sizes often follow a

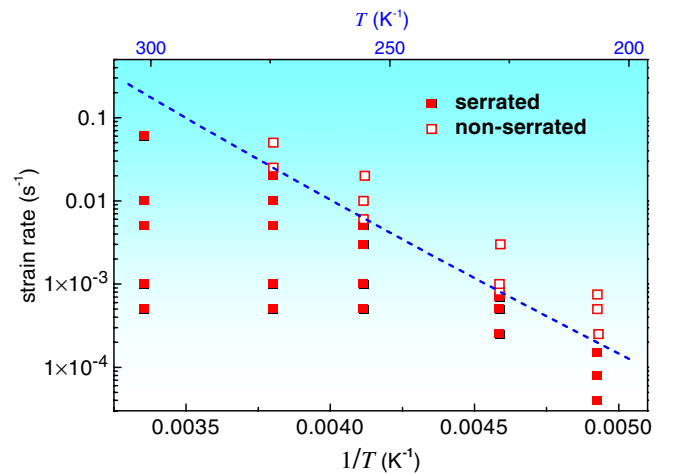


FIG. 4 (color online). The transition from serrated to nonserrated flow with the variation of strain rate at different temperatures for the $\text{Zr}_{65}\text{Ni}_{10}\text{Cu}_{15}\text{Al}_{10}$ BMG sample ($d = 2 \text{ mm}$), which can be well fitted by Eq. (9) (the dashed line).

power-law distribution, indicating the shear band interaction term or more degrees of freedom must be considered in the stick-slip dynamics of multiple shear bands. This may lead to the complex serrated events or self-organized critical avalanche dynamics [22,39]. But the critical condition for the instability should be the same as that of one single shear band. That is, both are associated with a negative strain rate sensitivity of the flow stress originated from the microscopic deformation mechanism of BMGs.

To conclude, we give an interpretation on the intermittent plastic flow behavior from the stick-slip shear band dynamics and the atomic-scale CSM model in BMGs. The good agreement between our theoretical analysis and the experimental results unambiguously demonstrates that the serrated flow is an intrinsic dynamic instability of shear band sliding in BMGs. Finally, it should be pointed out that intermittent plastic flow process has been widely observed in other disordered material (granular media, colloids, etc.), our theoretical method on the serrated flow in BMG may also be useful in analyzing the shear stability and dynamics of these disorder solids.

The authors thank S. Donath, M. Ferry, and K. K. Song for technical assistance and G. Wang at Shanghai University for stimulating discussions. This work was sponsored by the German Science Foundation under the Leibniz Program (Grant No. EC 111/26-1) and the NSF of China (Grant No. 51271195). J. Hu acknowledges the support from Research Foundation for Youth Scholars of Beijing Technology and Business University (QNJJ2012-32).

*Corresponding author.

ifwsun@gmail.com

- [1] S. Nasuno, A. Kudrolli, and J. P. Gollub, *Phys. Rev. Lett.* **79**, 949 (1997).
- [2] C. Drummond and J. Israelachvili, *Phys. Rev. E* **63**, 041506 (2001).
- [3] A. Lemaître, *Phys. Rev. Lett.* **89**, 195503 (2002).
- [4] V. V. Bulatov and A. S. Argon, *Model. Simul. Mater. Sci. Eng.* **2**, 167 (1994).
- [5] M. L. Falk and J. S. Langer, *Phys. Rev. E* **57**, 7192 (1998).
- [6] C. Maloney and A. Lemaître, *Phys. Rev. Lett.* **93**, 016001 (2004).
- [7] F. Spaepen, *Acta Metall.* **25**, 407 (1977).
- [8] A. S. Argon, *Acta Metall.* **27**, 47 (1979).
- [9] E. Bouchbinder, J. S. Langer, and I. Procaccia, *Phys. Rev. E* **75**, 036107 (2007).
- [10] W. L. Johnson and K. Samwer, *Phys. Rev. Lett.* **95**, 195501 (2005).
- [11] C. A. Schuh, *Acta Mater.* **55**, 4067 (2007).
- [12] M. W. Chen, *Annu. Rev. Mater. Res.* **38**, 445 (2008).
- [13] D. Ma, A. D. Stoica, X.-L. Wang, Z. P. Lu, B. Clausen, and D. W. Brown, *Phys. Rev. Lett.* **108**, 085501 (2012).
- [14] W. L. Johnson, *MRS Bull.* **24**, 42 (1999).
- [15] W. H. Wang, C. Dong, and C. H. Shek, *Mater. Sci. Eng. R* **44**, 45 (2004).
- [16] M. W. Chen, *NPG Asia Mater.* **3**, 82 (2011).
- [17] J. J. Lewandowski and A. L. Greer, *Nat. Mater.* **5**, 15 (2005).
- [18] M. W. Chen, A. Inoue, W. Zhang, and T. Sakurai, *Phys. Rev. Lett.* **96**, 245502 (2006).
- [19] R. Huang, Z. Suo, J. H. Prevost, and W. D. Nix, *J. Mech. Phys. Solids* **50**, 1011 (2002).
- [20] W. J. Wright, R. B. Schwarz, and W. D. Nix, *Mater. Sci. Eng. A* **319–321**, 229 (2001).
- [21] S. X. Song, H. Bei, J. Wadsworth, and T. G. Nieh, *Intermetallics* **16**, 813 (2008).
- [22] B. A. Sun, H. B. Yu, W. Jiao, H. Y. Bai, D. Q. Zhao, and W. H. Wang, *Phys. Rev. Lett.* **105**, 035501 (2010).
- [23] K. Wang, T. Fujita, Y. Q. Zeng, N. Nishiyama, A. Inoue, and M. W. Chen, *Acta Mater.* **56**, 2834 (2008).
- [24] R. Maaß, D. Klaumünzer, G. Villard, P. M. Derlet, and J. F. Löffler, *Appl. Phys. Lett.* **100**, 071904 (2012).
- [25] A. Dubach, F. H. D. Torre, and J. F. Löffler, *Acta Mater.* **57**, 881 (2009).
- [26] A. Vingradov, A. Lazarev, D. V. Louzguine-Luzgin, Y. Yokoyama, S. Li, A. R. Yavari, and A. Inoue, *Acta Mater.* **58**, 6736 (2010).
- [27] Z. Han, W. F. Wan, Y. Li, Y. J. Wei, and H. J. Gao, *Acta Mater.* **57**, 1367 (2009).
- [28] Z. Y. Liu, Y. Yang, and C. T. Liu, *Appl. Phys. Lett.* **99**, 171904 (2011).
- [29] P. G. Debendetti and F. H. Stillinger, *Nature (London)* **410**, 259 (2001).
- [30] D. Pan, A. Inoue, T. Sakurai, and M. W. Chen, *Proc. Natl. Acad. Sci. U.S.A.* **105**, 14769 (2008).
- [31] B. A. Sun, S. Pauly, J. Tan, M. Stoica, W. H. Wang, U. Kühn, and J. Eckert, *Acta Mater.* **60**, 4160 (2012).
- [32] See Supplemental Material at <http://link.aps.org/supplemental/10.1103/PhysRevLett.110.225501> for theoretical analysis and experimental details, Table SI and Figs. S1–S8.
- [33] D. Klaumünzer, R. Maaß, and J. F. Löffler, *J. Mater. Res.* **26**, 1453 (2011).
- [34] J. R. Rice and A. L. Ruina, *J. Appl. Mech.* **50**, 343 (1983).
- [35] A. L. Ruina, *J. Geophys. Res.* **88**, 10359 (1983).
- [36] J. S. Langer, *Phys. Rev. E* **70**, 041502 (2004).
- [37] E. G. Daub and J. M. Carlson, *Phys. Rev. E* **80**, 066113 (2009).
- [38] T. K. Haxton, and A. J. Liu, *Phys. Rev. Lett.* **99**, 195701 (2007).
- [39] K. A. Dahmen, Y. Ben-Zion, and J. T. Uhl, *Nat. Phys.* **7**, 554 (2011).